Analysis of two-dimensional photonic band gap structure with a rhombus lattice

Limei Qi (亓丽梅), Ziqiang Yang (杨梓强), Xi Gao (高 喜), and Zheng Liang (梁 正)

School of Physical Electronics, University of Electronic Science and Technology of China, Chengdu 610054

The relative band gap for a rhombus lattice photonic crystal is studied by plane wave expansion method and high frequency structure simulator (HFSS) simulation. General wave vectors in the first Briliouin zone are derived. The relative band gap as a function of air-filling factor and background material is investigated, respectively, and the nature of photonic band gap for different lattice angles is analyzed by the distribution of electric energy. These results would provide theoretical instruction for designing optical integrated devices using photonic crystal with a rhombus lattice.

OCIS codes: 160.4670, 230.0230, 230.3120, 220.0220.

Two-dimensional (2D) photonic crystal (PC) has attracted considerable attention owing to its remarkable features[1,2]. One of the most attractive applications is its usage for the realization of high-density photonic integrated circuits (PICs)[3]. However, the PC devices are limited because most studies are based on PC with triangular, square or rectangular lattice[4,5]. Photonic band gap (PBG) of metallic PC with a rhombus lattice has been discussed by transmission matrix method[6]. In this letter, the relative band gap $\omega_R = \Delta\omega/\omega_g$[7] (where ω_g is the frequency at the middle gap, and $\Delta\omega$ the frequency width of the gap) in the first PBG for a rhombus lattice PC is analyzed by plane wave expansion method and high frequency structure simulator (HFSS) simulation, and the nature of PBG for different lattice angles is also analyzed by the distribution of electric energy.

Figure 1(a) shows a PC structure with a rhombus lattice made of circular scatter in background material. ε_a is the relative dielectric constant for circular scatter, and ε_b is that of the background material. a is the length of the rhombus lattice, and θ is the lattice angle of the sharp corner. When θ is equal to $60°$ or $90°$, a triangular or square lattice PC could be formed. In this letter, it is worth noting that θ considered here changes from $0°$ to $90°$ with interval of $10°$, and some curves of ω_R for certain lattice angle are not shown since their values are too small to be considered.

Primitive lattice vectors $(\mathbf{a}_1, \mathbf{a}_2)$ and reciprocal lattice vector $\mathbf{G}$ for the rhombus lattice PC are given by

$$\mathbf{a}_1 = a\mathbf{e}_x,$$

$$\mathbf{a}_2 = a(\cos\theta\mathbf{e}_x + \sin\theta\mathbf{e}_y),$$

$$\mathbf{G} = \frac{2\pi}{a}h_1\mathbf{e}_x + \frac{2\pi}{a}(\frac{h_2}{\sin\theta} - h_1\mathrm{ctg}\theta)\mathbf{e}_y, \quad (1)$$

with $\mathbf{e}_x$, $\mathbf{e}_y$ the unit vectors, and h_1, h_2 integers, respectively.

Figure 1(b) shows the first Brillouin zone (BZ) of a rhombus lattice PC structure. Appling the boundary condition in the first BZ[8]

$$\mathbf{G} \cdot (\mathbf{k} + \frac{\mathbf{G}}{2}) = 0, \quad (2)$$

wave vectors $\mathbf{k}$ in each point are derived as follows:

$$\mathbf{k}_\Gamma = (0,0),$$

$$\mathbf{k}_T = \frac{\pi}{a}(1, \frac{1-\cos\theta}{\sin\theta}),$$

$$\mathbf{k}_N = \frac{\pi}{a}(1 - \frac{1-\cos\theta}{\sin\theta}\mathrm{ctg}\theta, \frac{1}{\sin\theta}),$$

$$\mathbf{k}_X = \frac{\pi}{a}(0, \frac{1}{\sin\theta}),$$

$$\mathbf{k}_M = \frac{\pi}{a}(\frac{1-\cos\theta}{\sin\theta}\mathrm{ctg}\theta - 1, \frac{1}{\sin\theta}),$$

$$\mathbf{k}_P = \frac{\pi}{a}(-1, \mathrm{ctg}\theta). \quad (3)$$

If wave vector $\mathbf{k}$ in the first BZ changes along

$$\Gamma \to T \to N \to \Gamma \to X \to M \to \Gamma \to P \to M,$$

PBG of a rhombus lattice PC for TM and TE modes can be achieved using plane wave expansion method[9].
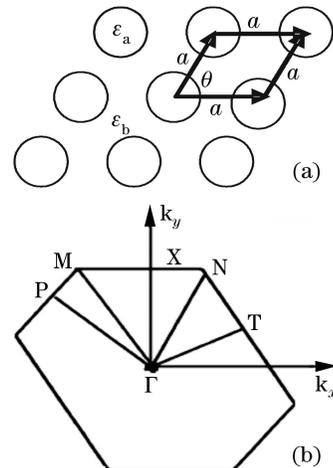

Fig. 1. PC structure with a rhombus lattice. (a) Primitive lattice space and (b) schematic view of the first Brillouin zone.

In our calculation, $441(10 \leq h_1, h_2 \leq 10)$ reciprocal vectors per unit cell are used and the convergence is better than 2%. For the fabrication and experimental point of view[10,11], rhombus lattice PC made of circular air holes in silicon (relative dielectric constant $\varepsilon_r = 11.9$) is considered.

The ω_R of TE and TM modes versus air-filling factor f for circular air holes in silicon with different lattice angle θ are shown in Figs. 2(a) and (b), respectively.

From Fig. 2(a), we can see that ω_R only appears in a certain range of air-filling factor f and lattice angle θ. When θ is fixed, ω_R for TE mode firstly increases from zero, then decreases after arriving at peak value with f adding. For 50°, 60° and 70°, the peak value appears at $f = 0.6$. The maximum value is obtained at $f = 0.55$ when θ is 80° and 90°. The biggest ω_R for TE mode is 0.502 at $f = 0.6$ and $\theta = 60°$. For TM mode, ω_R only appears at large lattice angle and increases at all time with f increasing when θ is fixed.

On the other hand, when air-filling factor f is fixed, ω_R increases with θ changing along $90° \rightarrow 80° \rightarrow 50° \rightarrow 70° \rightarrow 60°$ for TE mode, and increasing along $70° \rightarrow 80° \rightarrow 90°$ for TM mode. This behavior can be understood by comparing the difference of the energy distribution at different lattice angles which are responsible for the splitting between the lowest two bands[9]. An appropriate measure of the degree of concentration of the displacement fields in the silicon regions is the fill factor, defined as[12]

$$F = \frac{\int\limits_{\text{silicon}} E^*(r) \cdot D(r) \mathrm{d}^2 r}{\int\limits_{\text{all place}} E^*(r) \cdot D(r) \mathrm{d}^2 r}, \quad (4)$$

where $E(r)$ and $D(r)$ are the electric field and displacement field, respectively. Tables 1 and 2 show the fill factors for TE and TM modes at the air-filling factor of 0.65,
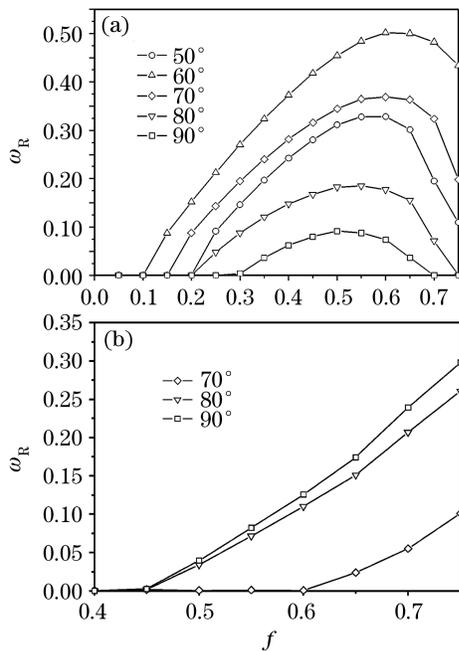
Table 1. Fill Factors for TE Mode

θ	F_1	F_2	ΔF	ω_R
90°	0.438	0.562	0.124	0.032
80°	0.514	0.384	0.130	0.155
50°	0.580	0.313	0.267	0.302
70°	0.595	0.192	0.403	0.363
60°	0.795	0.178	0.617	0.500

Table 2. Fill Factors for TM Mode

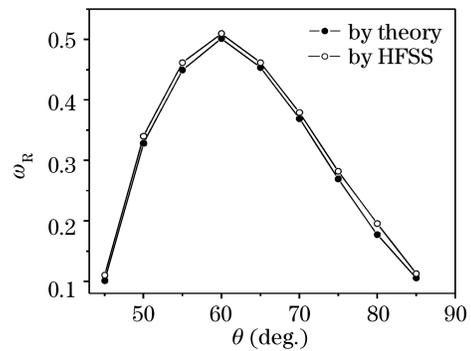| θ	F_1	F_2	ΔF	ω_R
50°	0.943	0.944	0.001	0
60°	0.945	0.947	0.002	0
70°	0.954	0.930	0.024	0.024
80°	0.974	0.855	0.119	0.151
90°	0.980	0.836	0.144	0.175

Fig. 3. Relative band gap ω_R versus lattice angle θ for air holes in silicon at the air-filling factor of 0.6.
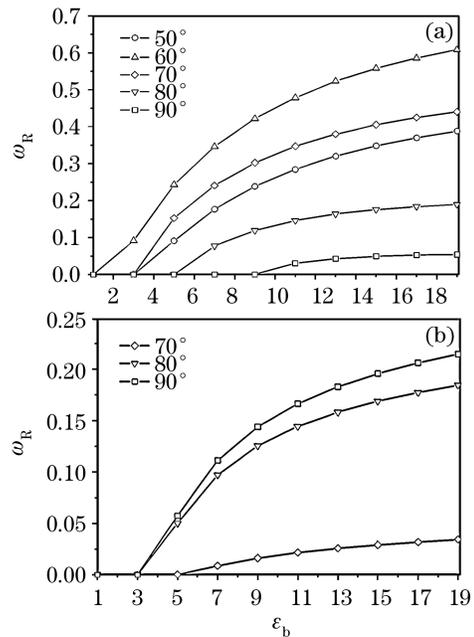

Fig. 4. Relative band gap ω_R versus background material ε_b for circular air holes in silicon at the air-filling factor of 0.65 (a) for TE mode and (b) for TM mode.

Fig. 2. Relative band gap ω_R versus air-filling factor f for circular air holes in silicon with a rhombus lattice (a) for TE mode and (b) for TM mode.

respectively. F_1 is the fill factor of the highest frequency in the first band and F_2 is the fill factor of the lowest

frequency in the second band. ΔF is the difference of electric energy between the lowest two bands. It is clear from Tables 1 and 2 that, for both TE and TM modes, the stronger the electrical energy contrast, the bigger the value of ω_R is.

To demonstrate the results of the theory above, ω_R of circular air holes in silicon at $f = 0.6$ are simulated using HFSS, which is a three-dimensional (3D) electromagnetic (EM) simulation software based on finite element method (FEM)[13,14]. Comparative results of ω_R versus θ for the two methods are shown in Fig. 3. It is obvious that ω_R simulated by HFSS are basically in accordance with what are calculated by plane wave method.

In order to investigate how the relative dielectric constant of the background material ε_b affects the relative band gap, ω_R versus ε_b at $f = 0.65$ is given in Fig. 4. Interestingly, ω_R increases with the increase of ε_b for both TE and TM modes at fixed θ. If ε_b is fixed, ω_R enlarges with θ along $90° \rightarrow 80° \rightarrow 50° \rightarrow 70° \rightarrow 60°$ for TE mode and $70° \rightarrow 80° \rightarrow 90°$ for TM mode.

In conclusion, the relative band gap ω_R of a rhombus lattice PC, for both TE and TM modes, is studied by plane wave method and HFSS simulation. When the lattice angle is fixed, ω_R firstly increases with f adding, and then decreases after arriving at peak value for TE mode. For TM mode, ω_R only exists at large lattice angle, and always increases with f adding. When f is fixed, ω_R enlarges with θ changing along $90° \rightarrow 80° \rightarrow 50° \rightarrow 70° \rightarrow 60°$ for TE mode and $70° \rightarrow 80° \rightarrow 90°$ for TM mode. The distribution of the electric energy is responsible for these trends. With the adding of relative dielectric constant of background material ε_b, ω_R always increases for both TE and TM modes. These results would provide theoretical instruction for designing optical integrated devices using PC with a rhombus lattice.

References

1. E. Yablonovitch, Phys. Rev. Lett. **58,** 2059 (1987).
2. S. John, Phys. Rev. Lett. **58,** 2486 (1987).
3. C. Manolatou, S. G. Johnson, S. Fan, P. R. Villeneuve, H. A. Haus, and J. D. Joannopoulos, J. Lightwave Technol. **17,** 1682 (1999).
4. J. Mizuguchi, Y. Tanaka, S. Tamura, and M. Notomi, Phys. Rev. B **67,** 075109 (2003).
5. Z. Liu, G. Zhou, and L. Hou, Chin. Opt. Lett. **4,** 566 (2006).
6. B. Hao, P. Liu, and C. Tang, Acta Phys. Sin. (in Chinese) **55,** 1862 (2006).
7. F. Wu, Z. Liu, and Y. Liu, Chin. Phys. Lett. **18,** 785 (2001).
8. H. Lin and S. Zhang, *Solid State Physics and Physical Measure* (in Chinese) (Science Press, Beijing; University of Science and Technology of China Press, Hefei, 2005) p.6.
9. J. D. Joannopoulos, R. D. Meade, and J. N. Winn, *Photonic Crystals: Molding the Flow of Light* (Princeton University Press, Princeton, 1995) pp.56 − 65.
10. M. Lončar, T. Doll, J. Vučković, and A. Scherer, J. Lightwave Technol. **18,** 1402 (2000).
11. Y. Jiang, J. Wei, L. Gu, X. Chen, and R. Chen, Appl. Phys. Lett. **87,** 221105 (2005).
12. R. D. Meade, A. M. Rappe, K. D. Brommer, and J. D. Joannopoulos, J. Opt. Soc. Am. B **10,** 328 (1993).
13. HFSS v9, *Getting Started with HFSS* (Ansoft Corporation, Pittsburgh, 2004).
14. J. D. Shumpert, W. J. Chappell, and L. P. B. Katehi, IEEE Trans. Microwave Theory and Techniques **47,** 2099 (1999).